Supporting Information

Modifying cell membranes with anionic polymer amphiphiles potentiates intracellular delivery of cationic peptides.

Eric A. Dailing[1], Kameron V. Kilchrist[1], J. William Tierney[1], R. Brock Fletcher[1], Brian C. Evans[1], and Craig L. Duvall[1,*].

[1]Department of Biomedical Engineering, Vanderbilt University, PMB 351634, Nashville TN 37235.

*Email: craig.duvall@vanderbilt.edu

Supplementary Figures

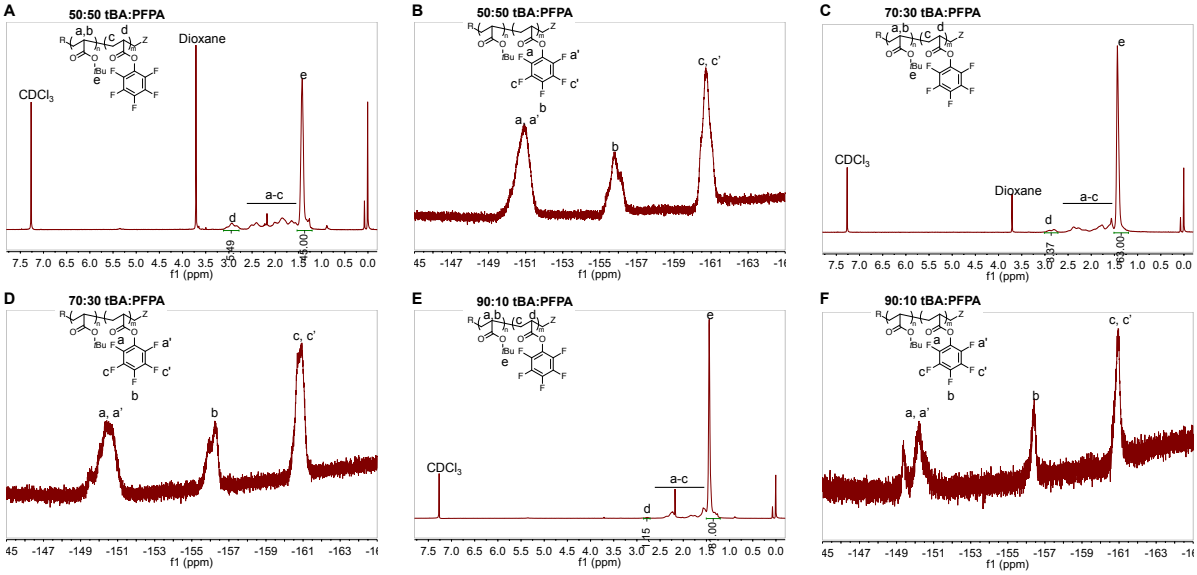

Figure S1. NMR spectra of parent polymers. A: 50:50 tBA:PFPA, ^{1}H. B: 50:50 tBA:PFPA, ^{19}F. C: 70:30 tBA:PFPA, ^{1}H. D: 70:30 tBA:PFPA, ^{19}F. E: 90:10 tBA:PFPA, ^{1}H. F: 90:10 tBA:PFPA, ^{19}F.

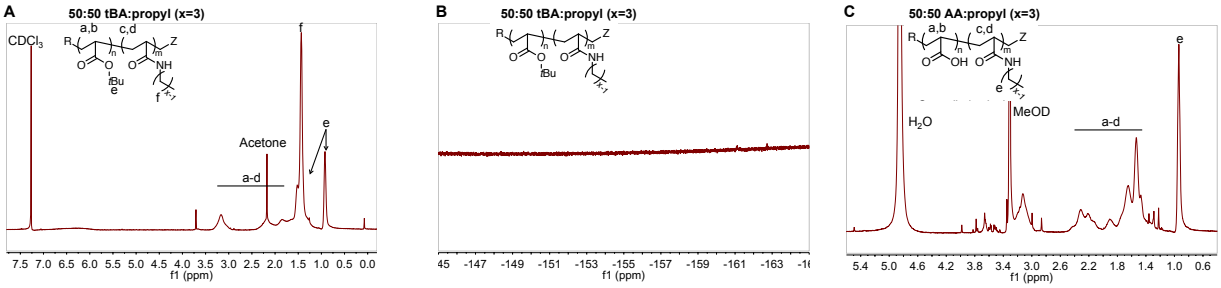

Figure S2. A: 50:50 tBA:propyl, ^{1}H, $CDCl_3$. B: 50:50 tBA: propyl, ^{19}F, $CDCl_3$. C: 50:50 AA:propyl, ^{1}H, MeOD.

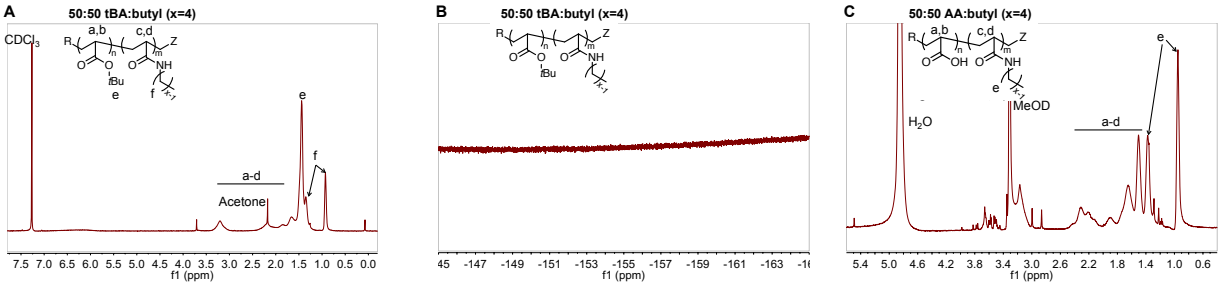

Figure S3. A: 50:50 tBA:butyl, ^{1}H, $CDCl_3$. B: 50:50 tBA:butyl, ^{19}F, $CDCl_3$. C: 50:50 AA:butyl, ^{1}H, MeOD.

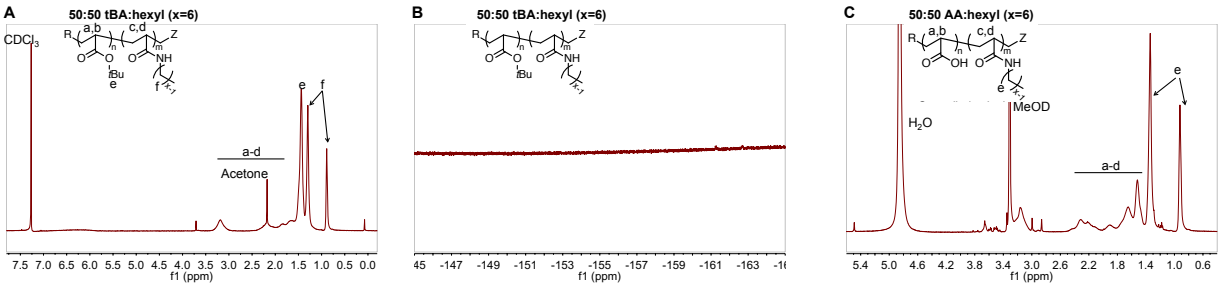

Figure S4. A: 50:50 tBA:hexyl, ^{1}H, $CDCl_3$. B: 50:50 tBA:hexyl, ^{19}F, $CDCl_3$. C: 50:50 AA:hexyl, ^{1}H, MeOD.

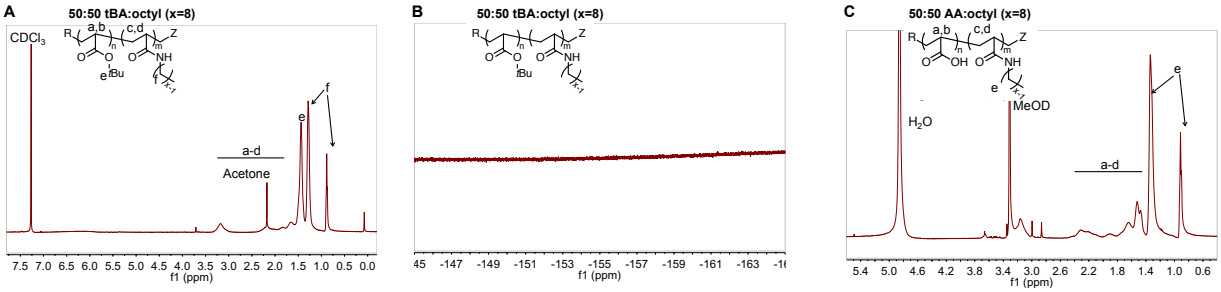

Figure S5. A: 50:50 tBA:octyl, ^{1}H, $CDCl_3$. B: 50:50 tBA:octyl, ^{19}F, $CDCl_3$. C: 50:50 AA:octyl, ^{1}H, MeOD.

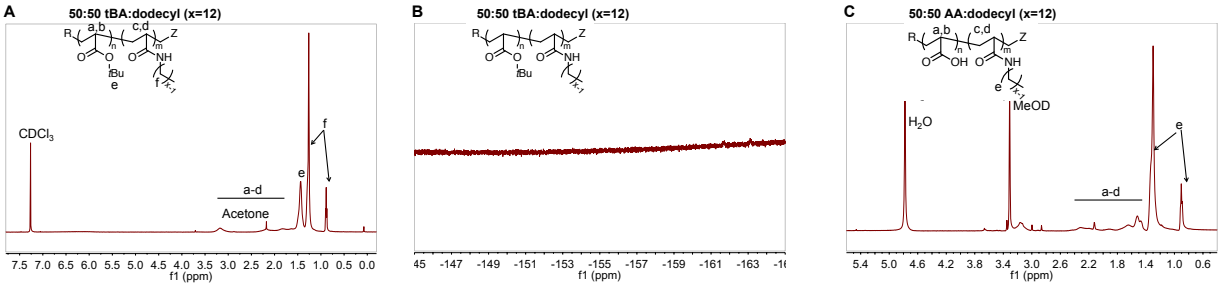

Figure S6. A: 50:50 tBA:dodecyl, ^{1}H, $CDCl_3$. B: 50:50 tBA:dodecyl, ^{19}F, $CDCl_3$. C: 50:50 AA:dodecyl, ^{1}H, MeOD.

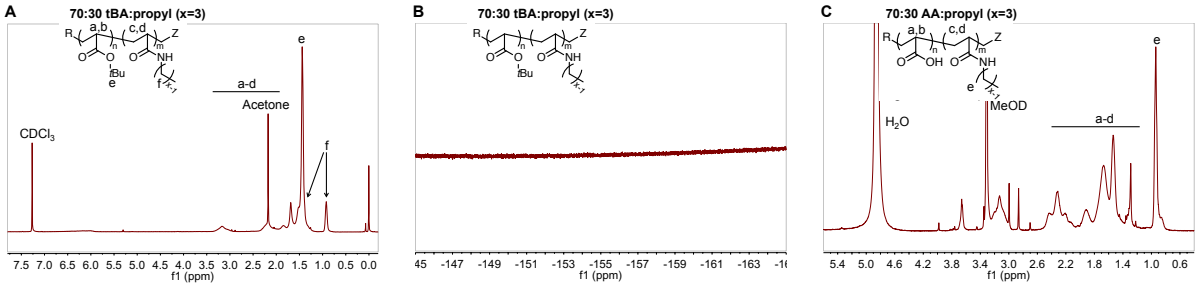

Figure S7. A: 70:30 tBA:propyl, ^{1}H, $CDCl_3$. B: 70:30 tBA:propyl, ^{19}F, $CDCl_3$. C: 70:30 AA:propyl, ^{1}H, MeOD.

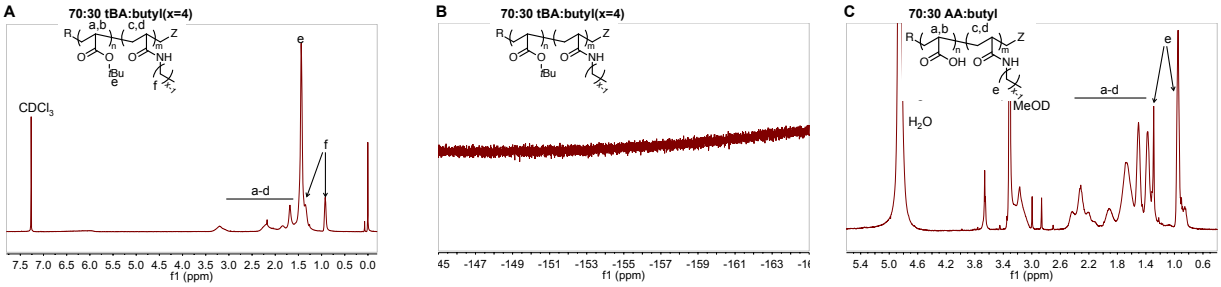

Figure S8. A: 70:30 tBA:butyl, ^{1}H, $CDCl_3$. B: 70:30 tBA:butyl, ^{19}F, $CDCl_3$. C: 70:30 AA:butyl, ^{1}H, MeOD.

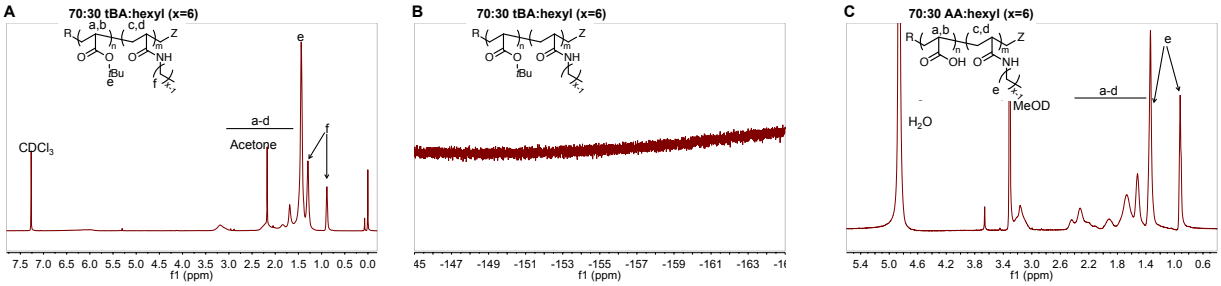

Figure S9. A: 70:30 tBA:hexyl, ^{1}H, $CDCl_3$. B: 70:30 tBA:hexyl, ^{19}F, $CDCl_3$. C: 70:30 AA:hexyl, ^{1}H, MeOD.

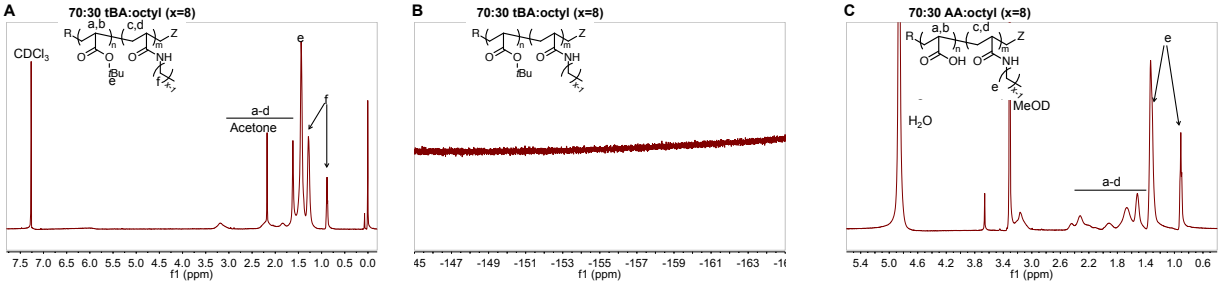

Figure S10. A: 70:30 tBA:octyl, ^{1}H, $CDCl_3$. B: 70:30 tBA:octyl, ^{19}F, $CDCl_3$. C: 70:30 AA:octyl, ^{1}H, MeOD.

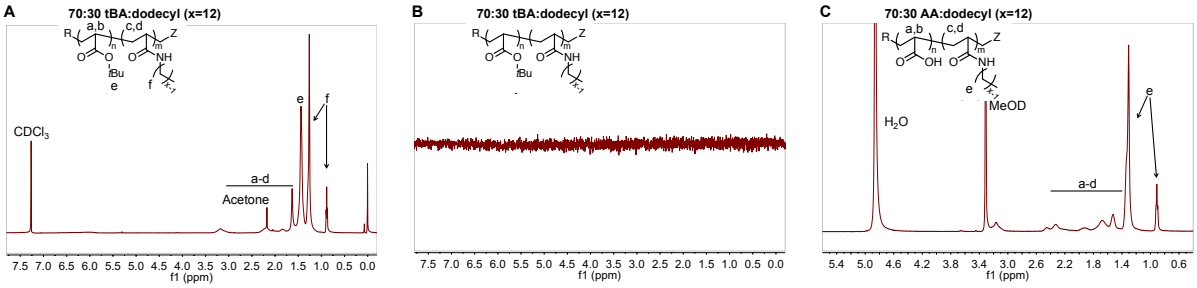

Figure S11. A: 70:30 tBA:dodecyl, ^{1}H, $CDCl_3$. B: 70:30 tBA:dodecyl, ^{19}F, $CDCl_3$. C: 70:30 AA:dodecyl, ^{1}H, MeOD.

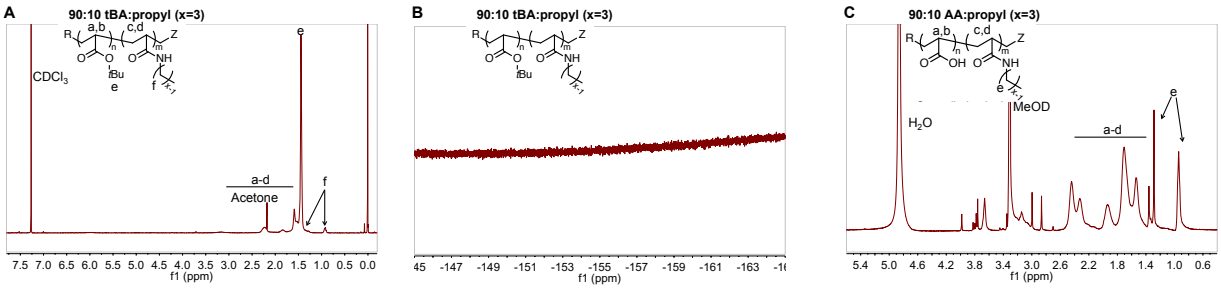

Figure S12. A: 90:10 tBA:propyl, ^{1}H, $CDCl_3$. B: 90:10 tBA:propyl, ^{19}F, $CDCl_3$. C: 90:10 AA:propyl, ^{1}H, MeOD.

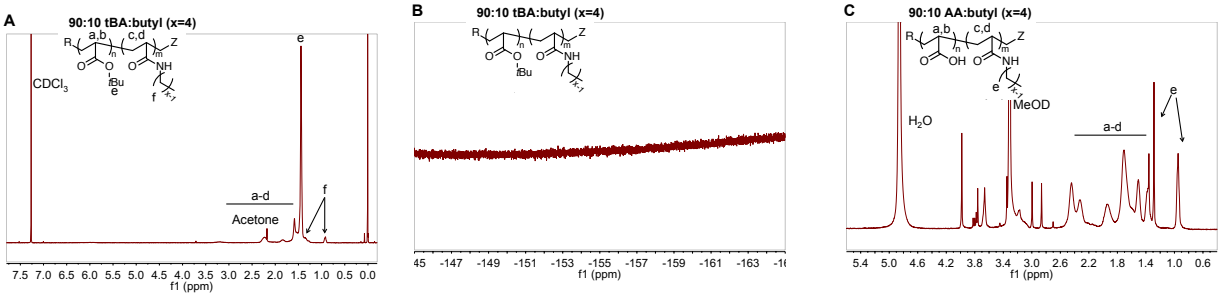

Figure S13. A: 90:10 tBA:butyl, ^{1}H, $CDCl_3$. B: 90:10 tBA:butyl, ^{19}F, $CDCl_3$. C: 90:10 AA:butyl, ^{1}H, MeOD.

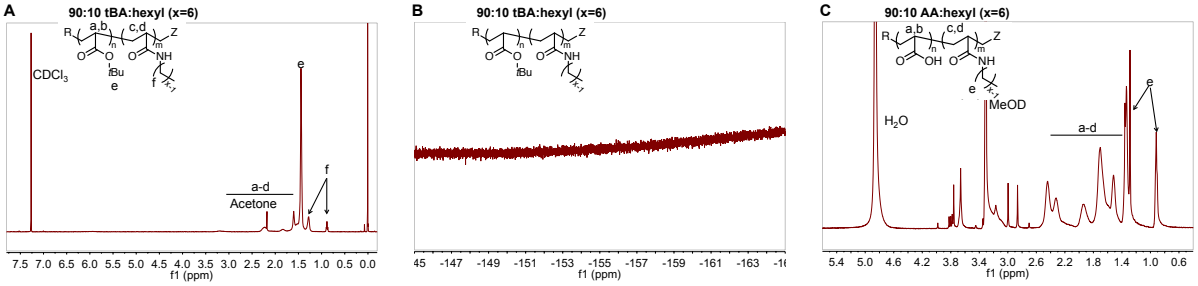

Figure S14. A: 90:10 tBA:hexyl, ^{1}H, $CDCl_3$. B: 90:10 tBA:hexyl, ^{19}F, $CDCl_3$. C: 90:10 AA:hexyl, ^{1}H, MeOD.

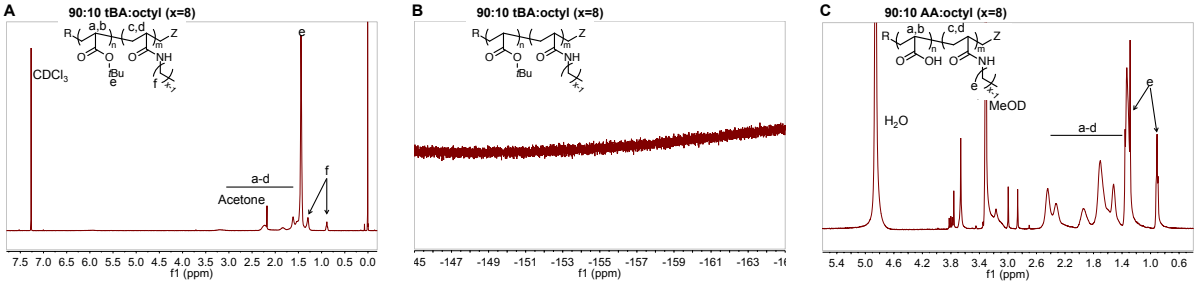

Figure S15. A: 90:10 tBA:octyl, ^{1}H, $CDCl_3$. B: 90:10 tBA:octyl, ^{19}F, $CDCl_3$. C: 90:10 AA:octyl, ^{1}H, MeOD.

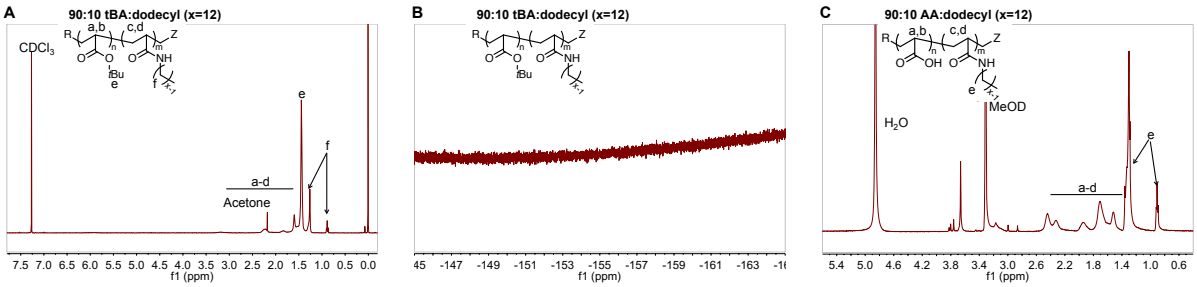

Figure S16. A: 90:10 tBA:dodecyl, ^{1}H, $CDCl_3$. B: 90:10 tBA:dodecyl, ^{19}F, $CDCl_3$. C: 90:10 AA:dodecyl, ^{1}H, MeOD.

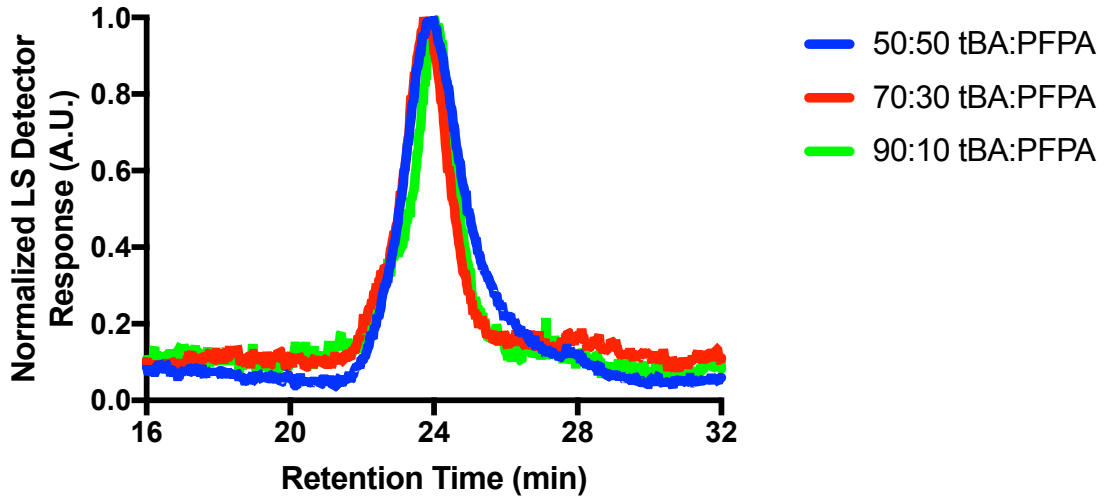

Figure S17. Gel permeation chromatography of tBA:PFPA polymers.

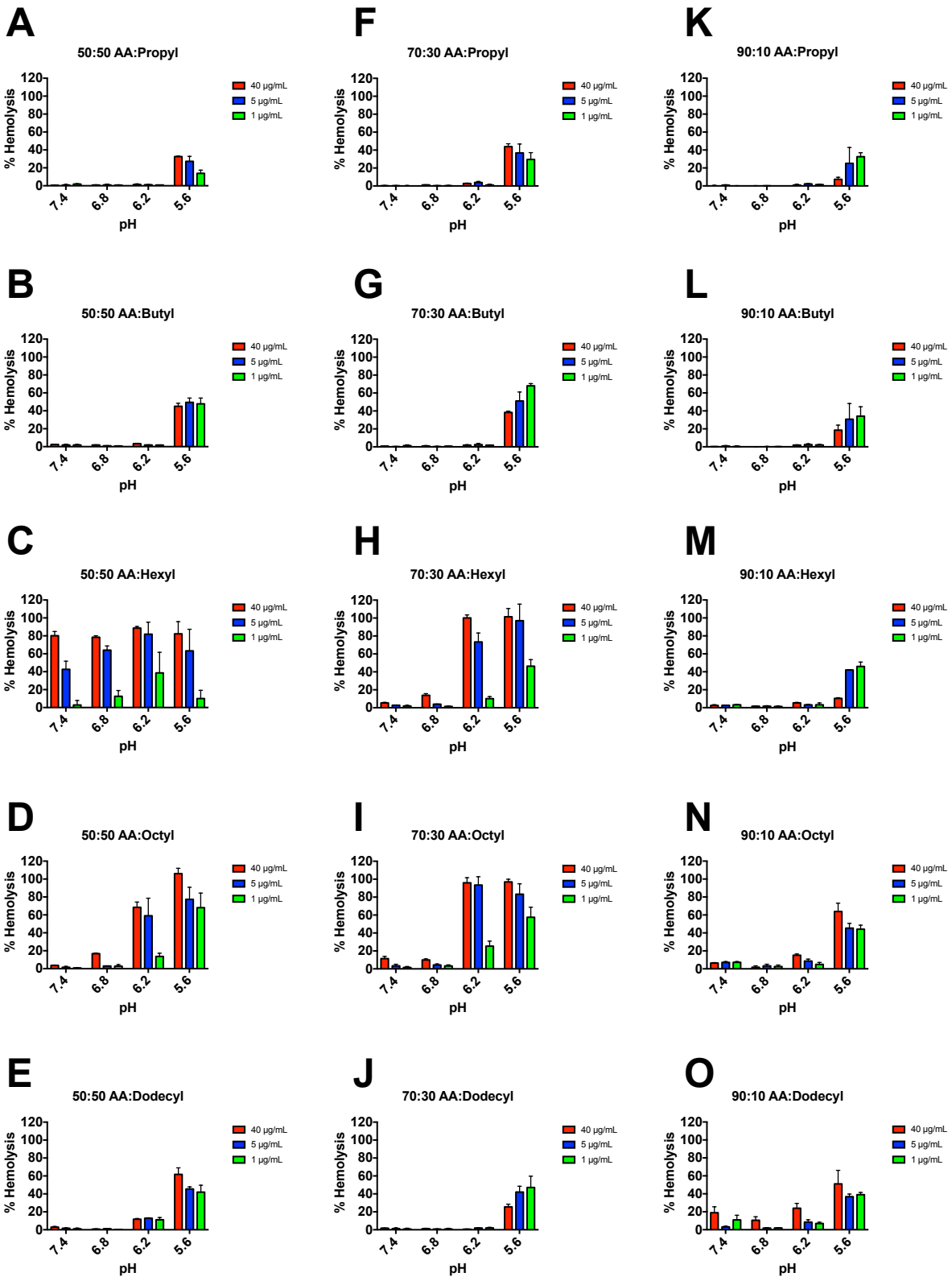

Figure S18. Red blood cell hemolysis of 50:50 (A-E), 70:30 (F-J), and 90:10 (K-O) AA:alkyl polymers as a function of pH and polymer concentration (n=3).

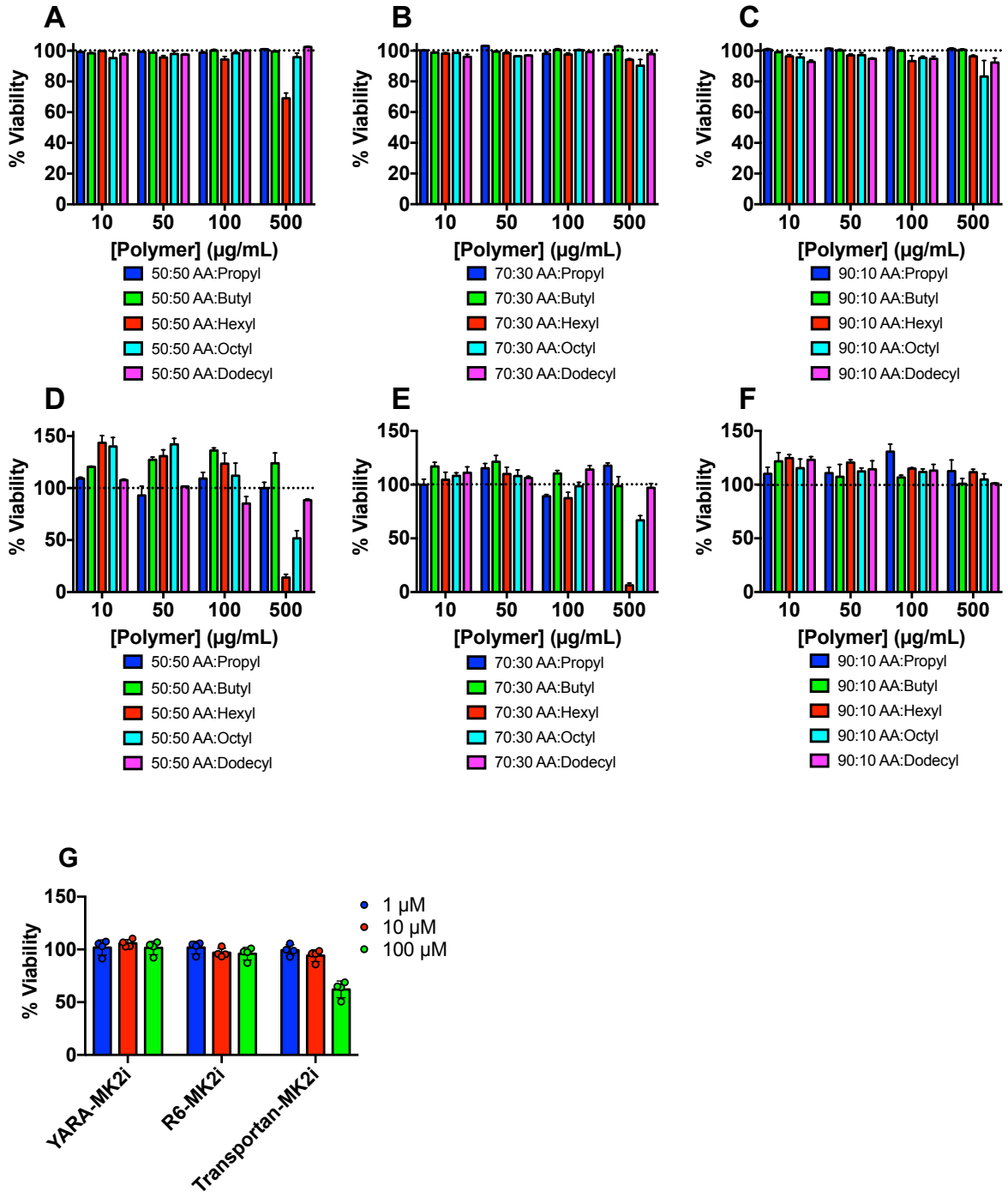

Figure S19. Polymer cytoxicity in A7r5 cells measured via Cell TiterGlo after treatment for 30 minutes followed by additional incubation for 0 h (A-C) or 24 h (D-E) as a function of concentration (n=3). Peptide cytotoxicity in A7r5 cells (G) measured via Cell TiterGlo after treatment for 30 minutes at 1, 10, and 100 μM (n=4).

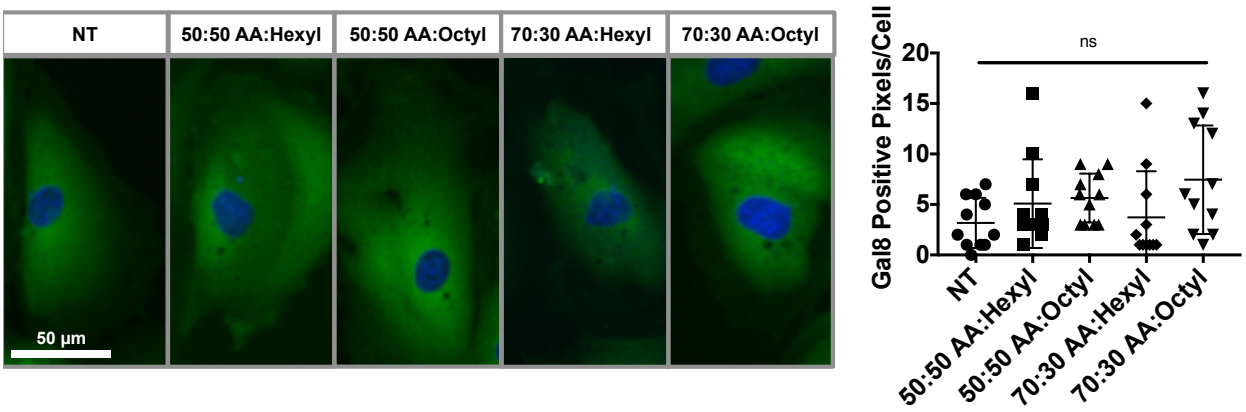

Figure S20. YFP-Gal8 reporter cells treated with BafA, followed by polymer, and imaged via confocal microscopy. Quantification of Gal8 positive punctate spots was performed in ImageJ (n=10). ns=p>0.05.

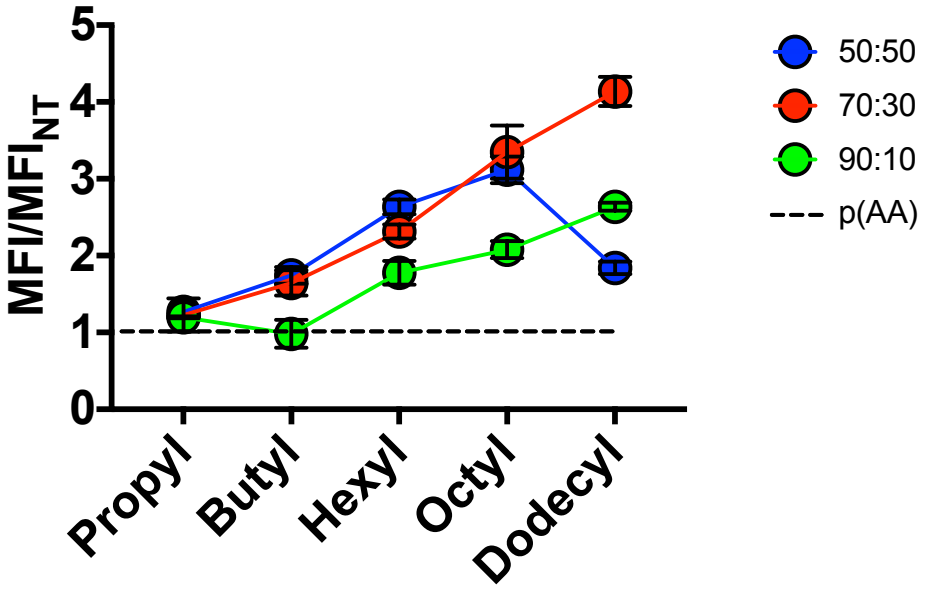

Figure S21. Intracellular uptake of A488-labeled polymers in A7r5 cells after 30 min treatment, normalized to untreated cells. MFI was normalized to individual polymer fluorescence to correct for differences in extent of fluorophore labeling (n=3).

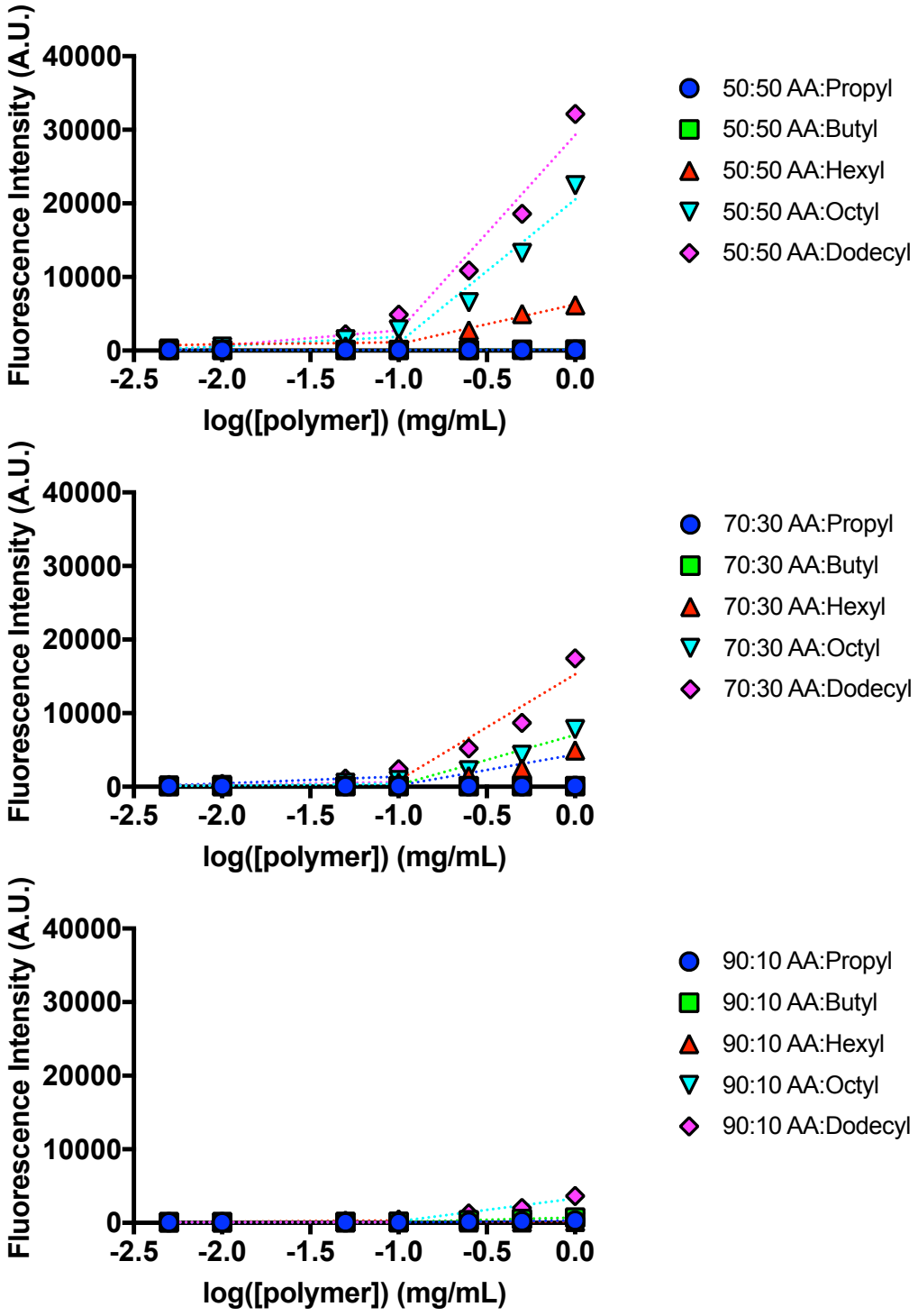

Figure S22. Fluorescence intensity of Nile red incubated with polymers at varying concentrations for 24 h (n=1).

Table S1. Concentrations at which the linear fits from the Nile red assay intersect, indicating the onset of aggregation. It is noteworthy that the magnitude of the Nile red fluorescence increases monotonically with increasing polymer hydrophobicity across all copolymer ratios, suggesting formation of hydrophobic domatins / aggregates. The increase in Nile red fluorescence at higher polymer concentration deviates from a linear fit for more hydrophobic polymers, which gives rise to some variability in fitting lines for the crossover concentration. Note that complementary dynamic light scattering analysis did not suggest that these polymers were actually forming a well-ordered micellar structure but more likely multimodal aggregates.

Polymer	Crossover Concentration (μg/mL)
50:50 AA:Propyl	**150**
50:50 AA:Butyl	**90.0**
50:50 AA:Hexyl	**92.5**
50:50 AA:Octyl	**111**
50:50 AA:Dodecyl	**101**
70:30 AA:Propyl	**-**
70:30 AA:Butyl	**-**
70:30 AA:Hexyl	**115**
70:30 AA:Octyl	**115**
70:30 AA:Dodecyl	**109**
90:10 AA:Propyl	**109**
90:10 AA:Butyl	**97.1**
90:10 AA:Hexyl	**-**
90:10 AA:Octyl	**118**
90:10 AA:Dodecyl	**108**

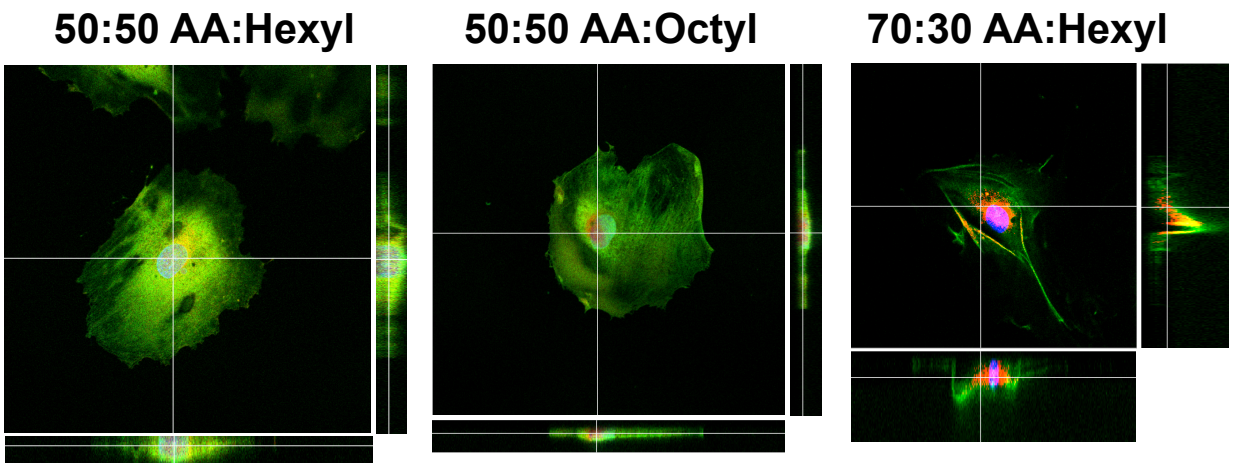

Figure S23. Confocal z-slices of A7r5 cells treated with A488 labeled polymer for 5 minutes. Nuclei are stained with DAPI, and cytoplasm is loaded with Calcein Orange-Red.

Supplemental Discussion

Cells were pre-treated with inhibitors covering a range of endocytosis pathways commonly implicated in the uptake of biomacromolecules and nanoparticles: wortmannin (macropinocytosis inhibitor), dynasore hydrate (dynamin-mediated endocytosis inhibitor), or methyl-β-cyclodextrin (lipid raft mediated endocytosis inhibitor)[1,2]. We then applied fresh media and added in treatments of fluorescently labeled polymer alone, labeled peptide alone, or sequential treatment of unlabeled polymer followed by labeled peptide. We focused this study on 70:30 AA:octyl and 50:50 AA:octyl, as both polymers enhance YARA and R6-MK2i uptake, are endosomolytic, and have different graft densities with equivalent alkyl length, while 50:50 AA:hexyl was omitted due to observing increased cytotoxicity of the endocytosis inhibitors when co-treated with this polymer. Uptake of YARA-MK2i peptide alone was inhibited in the presence of wortmannin and dynasore, indicating uptake via macropinocytosis and dynamin-mediated endocytosis, which is consistent with previous reports[2,3]. Uptake in cells sequentially treated with 70:30 AA:octyl and labeled YARA-MK2i peptide (Figure S24A) decreased only in the presence of dynasore, which suggests that a synergistic polymer-peptide interaction induced uptake via dynamin-mediated endocytosis. Sequential treatment with 50:50 AA:octyl on the other hand resulted in a decrease in uptake in the presence of wortmannin or dynasore, indicating that the more hydrophobic polymer also initiates uptake through macropinocytosis.

These experiments were repeated with R6-MK2i (Figure S24B) using the same conditions to examine the effects of peptide CPP chemistry on uptake mechanism. Only wortmannin inhibited uptake of R6-MK2i peptide alone, while sequential treatment of polymer and peptide produced a significant decrease in uptake in the presence of wortmannin or methyl β-cyclodextrin for both 70:30 and 50:50 AA:octyl polymers. These results suggest that peptide-

polymer interactions between R6-MK2i and these two polymers induce uptake through macropinocytosis and lipid-raft mediated endocytosis. The inclusion of competitive ligands for these endocytosis inhibitors as a further control was not possible due to confounding interactions with polymer and peptide, so these data are most appropriately interpreted for the relative differences in uptake pathway as a function of polymer and peptide structure. Overall, this set of experiments indicates that polymers that stably coat the cell membrane drive peptide internalization (Figure 2A,B and Figure 4B), polymer treatment does not permit passive diffusion of larger biomolecules (Figure 5), polymer-enhanced peptide uptake occurs through multiple pathways, and the relative influence of each pathway is dependent on both polymer and peptide structure (Figure S24).

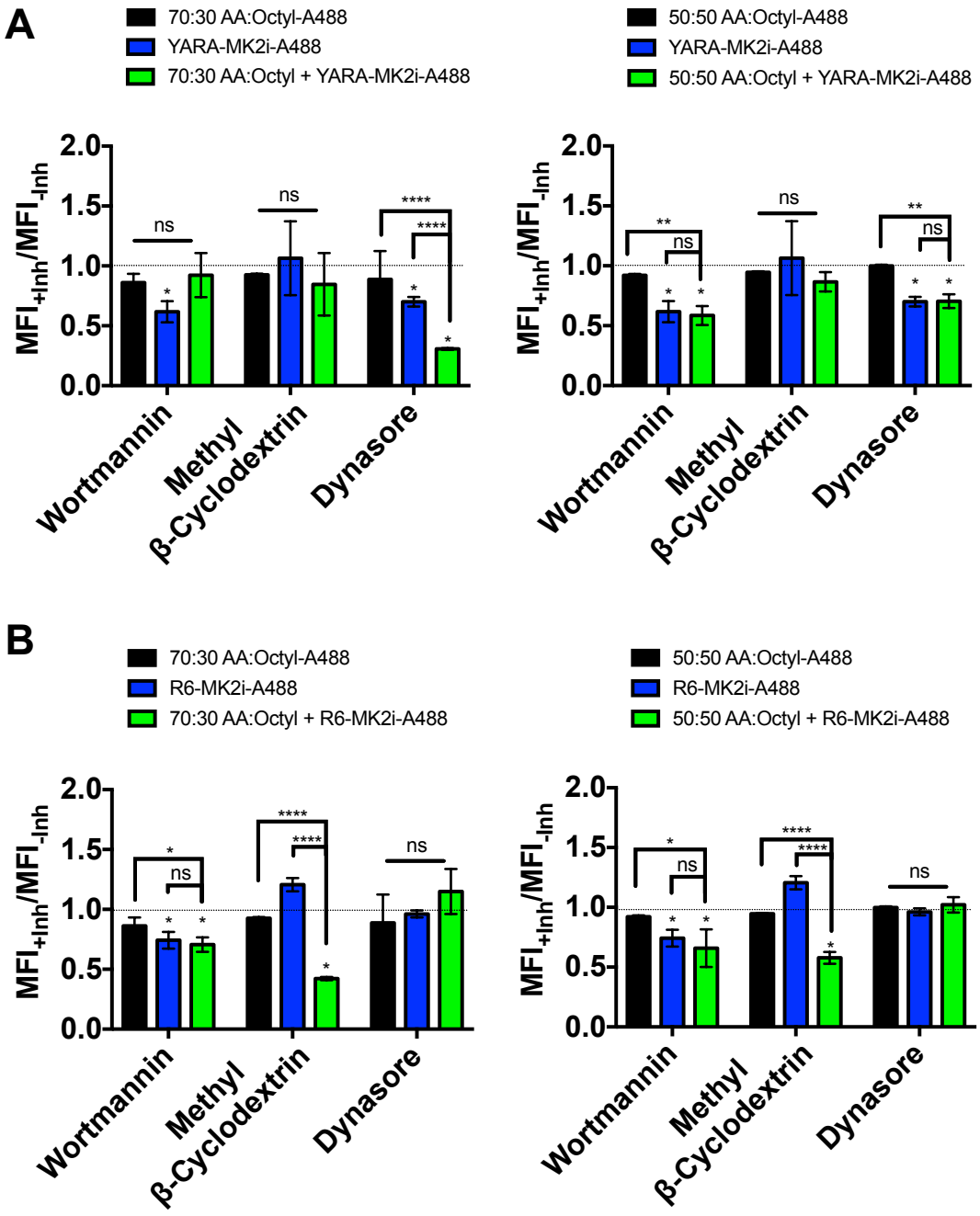

Figure S24. Polymer-peptide interactions at the cell membrane enhance peptide endocytosis through multiple pathways. Fold change in mean fluorescence intensity of A7r5 cells pretreated with a series of endocytosis inhibitors, followed by individual treatment of AlexaFluor-488 labeled polymer, AlexaFluor-488 labeled YARA-MK2i (A) or R6-MK2i (B), or sequential unlabeled polymer followed by the indicated AlexaFluor-488 labeled peptide (n=3). Individual markers above each bar indicate significant inhibition. *=$p<0.05$, **=$p<0.01$, ****=$p<0.0001$, ns=$p>0.05$.

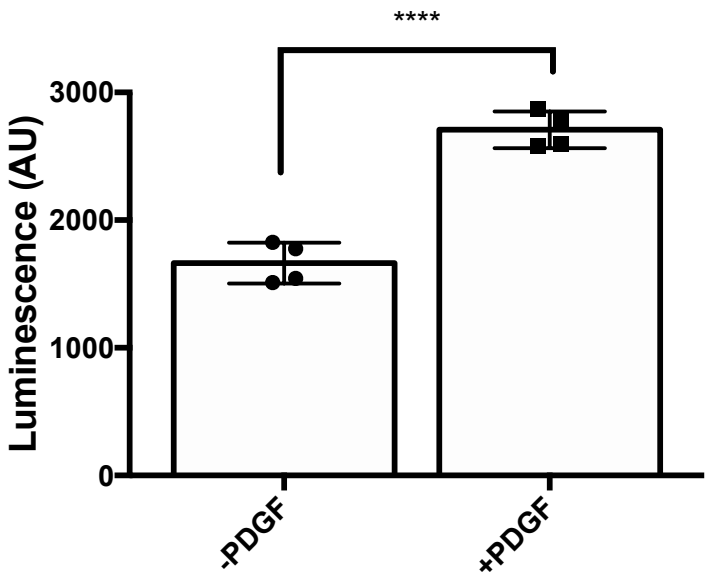

Figure S25. CREB-luc positive A7r5 cells stimulated with 20 ng/mL PDGF for 18 h compared to unstimulated cells (-PDGF) (n=4). **** = $p<0.0001$

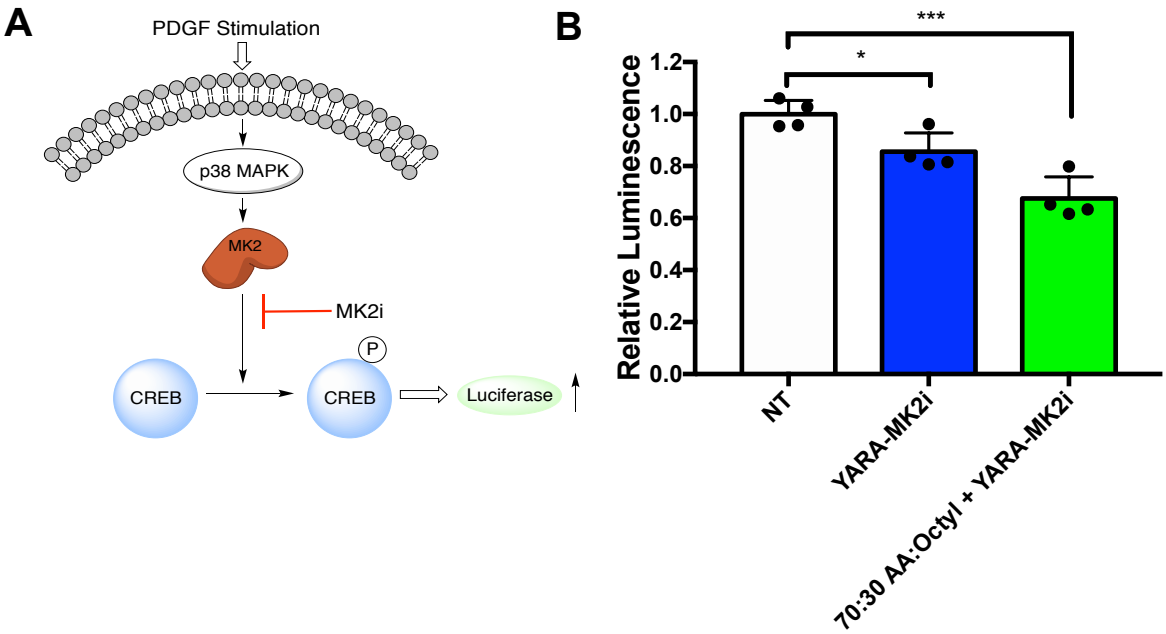

Figure S26. A) Schematic of MK2i-mediated inhibition of luciferase expression following PDGF stimulation. B) Relative luminescence of CREB-luc positive A7r5 cells following YARA-MK2i or polymer + YARA-MK2i pre-treatment and PDGF stimulation (n=4). *=$p<0.05$, ***=$p<0.001$

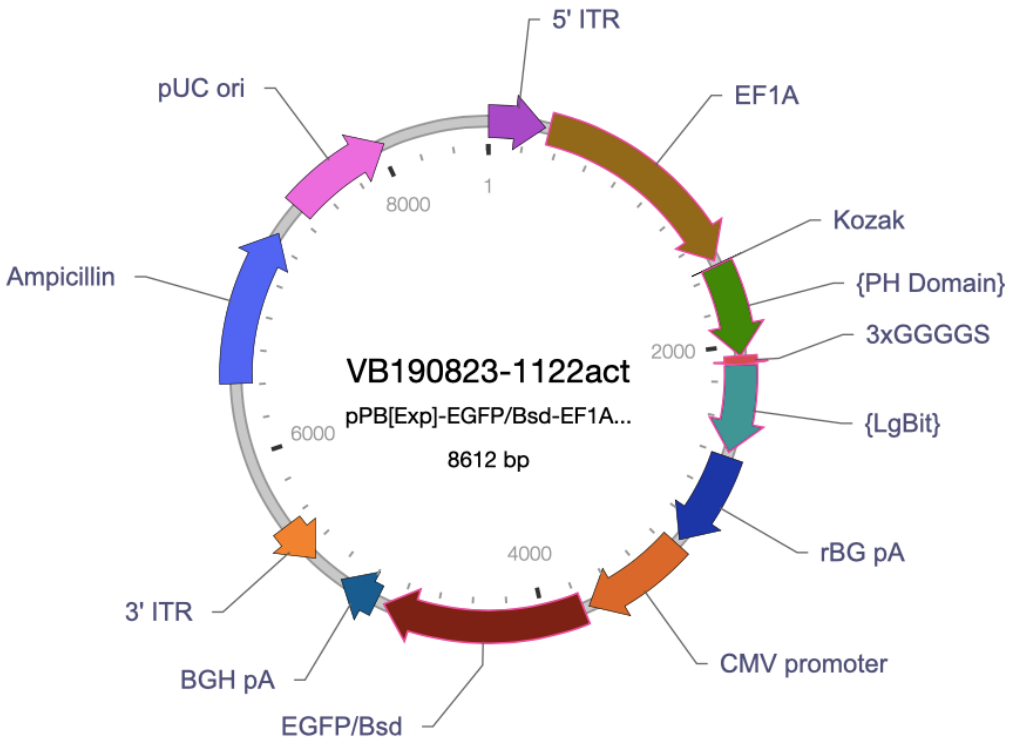

Figure S27. Map of the plasmid used to generate the HEK 293-T LgBiT cell line.

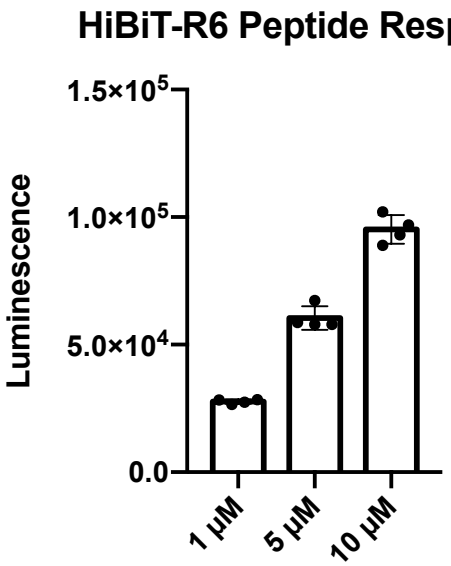

Figure S28. Luminescence of LgBiT-positive HEK-293T cells treated with 1, 5, or 10 µM HiBiT-R6 peptide followed by luciferase substrate (n=4).

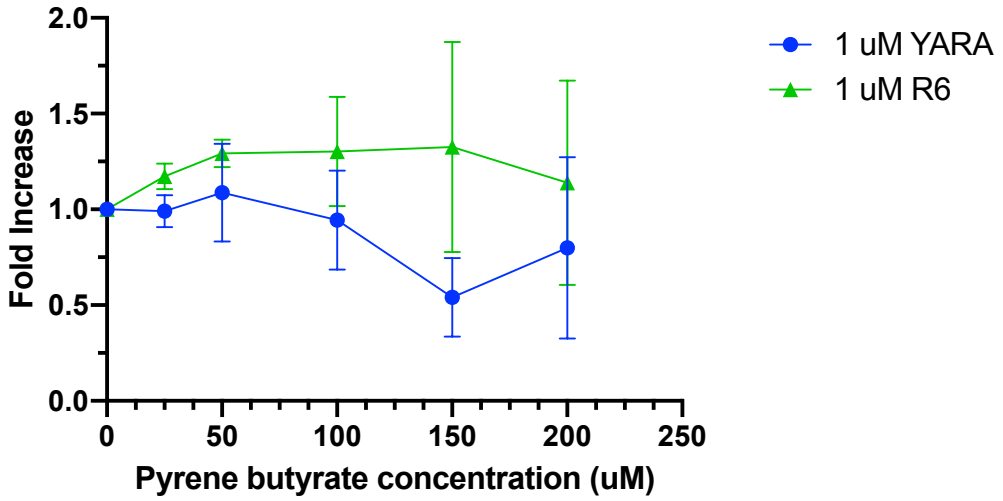

Figure S29. Fold change in luminescence of LgBiT-positive HEK-293T cells treated with the indicated dose of pyrene butyrate for 5 minutes, followed by incubation with 1 μM YARA or R6-HiBiT peptide for 2 h (n=4).

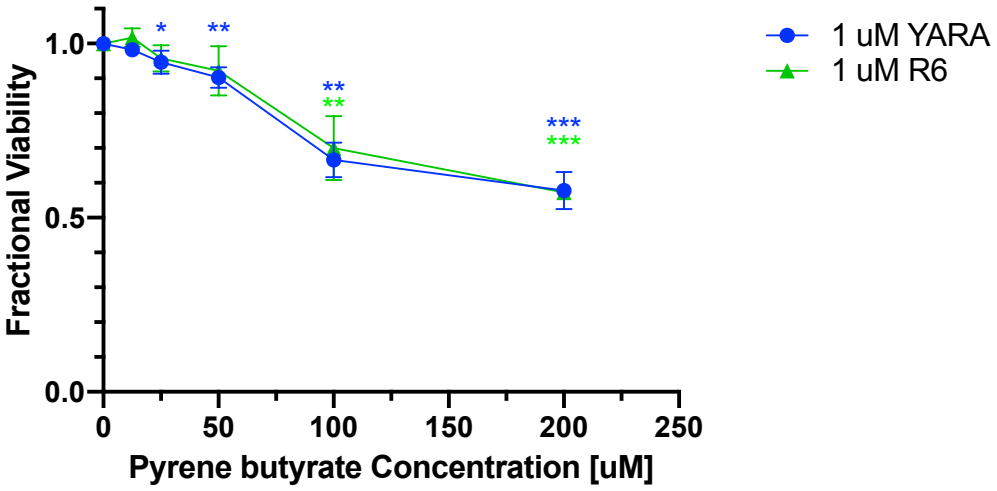

Figure S30. Fractional viability of LgBiT-positive HEK-293T cells treated with the indicated dose of pyrene butyrate for 5 minutes, followed by incubation with 1 μM YARA or R6-HiBiT peptide for 2 h (n=4). *=p<0.05, **=p<0.01, ***=p<0.001

Table S2. Amino acid sequence of reported cell penetrating sequences and net charge of CPP-MK2i and CPP-HiBiT. *a*: Total charge/number of amino acids in CPP. *b*: Hopp&Woods hydrophilicity scale, which ranks amino acids based on their water solubility. Percentage is the fraction of hydrophilic amino acids/total number of amino acids.

Peptide	Sequence	Net Charge	Charge Density[a]	Isoelectric Point	Average Hydrophilicity[b]
YARA-MK2i	YARAAARQARA-KALARQLGVAA	+5	0.227	12.4	0.1 (32%)
TAT-MK2i	GRKKRRQRRRPPQ - KALARQLGVAA	+10	0.4	12.9	1.0 (54%)
R6-MK2i	RRRRRR-KALARQLGVAA	+8	0.471	12.9	1.0 (53%)
Penetratin-MK2i	RQIKIWFQNRRMKWKK-KALARQLGVAA	+9	0.333	12.6	0.1 (46%)
Transportan-MK2i	GWTLNSAGYLLGKINLKALAALAKKIL-KALARQLGVAA	+6	0.158	11.3	-0.3 (26%)
YARA-HiBiT	YARAAARQARA-VSGWRLFKKIS	+6	0.273	12.5	0.2 (45%)
R6-HiBiT	RRRRRR - VSGWRLFKKIS	+9	0.529	13.3	1.0 (71%)

Supplemental References

(1) Falcone, S.; Cocucci, E.; Podini, P.; Kirchhausen, T.; Clementi, E.; Meldolesi, J. Macropinocytosis: Regulated Coordination of Endocytic and Exocytic Membrane Traffic Events. *J. Cell Sci.* **2006**, *119* (22), 4758–4769. https://doi.org/10.1242/jcs.03238.

(2) Brugnano, J.; Mcmasters, J.; Panitch, A. Characterization of Endocytic Uptake of MK2-Inhibitor Peptides. *J. Pept. Sci.* **2013**, *19* (10), 629–638. https://doi.org/10.1002/psc.2541.

(3) Kilchrist, K. V.; Evans, B. C.; Brophy, C. M.; Duvall, C. L. Mechanism of Enhanced Cellular Uptake and Cytosolic Retention of MK2 Inhibitory Peptide Nano-Polyplexes. *Cell. Mol. Bioeng.* **2016**, *9* (3), 368–381. https://doi.org/10.1007/s12195-016-0446-7.